PROCEEDINGS OF SCIENCE

Higher-Order Electroweak Contributions to Indirect CP Violation in Neutral Kaons

Joachim Brod,[a] **Sandra Kvedaraitė,**[a] **Zachary Polonsky**[a,b,*] **and Ahmed Youssef**[a]

[a] *University of Cincinnati,*
2600 Clifton Ave., Cincinnati, OH 45221, USA
[b] *Universität Zürich,*
Rämistrasse 71, Zürich, Switzerland

E-mail: zach.polonsky@physik.uzh.ch

The parameter ϵ_K is an important measure of the imbalance between matter and antimatter in the neutral kaon (K^0 and $\bar{K}^0$) system. In particular, ϵ_K provides a highly sensitive probe of new physics and plays a critical role in the global fit of the Cabibbo-Kobayashi-Maskawa matrix. As one of the first discovered sources of CP violation, it has been extensively measured in experiment to per-mil precision. The theoretical calculation of ϵ_K, however, has historically been plagued by large perturbative errors arising from charm-quark corrections. These errors were larger than the expected magnitude of higher-order electroweak corrections in perturbation theory, rendering these contributions irrelevant. Recently, it was discovered that a simple re-parameterization of the effective Hamiltonian drastically reduces perturbative errors, making these higher-order electroweak calculations worth-while. We present the $O(1\%)$ next-to-leading-logarithm electroweak contributions to ϵ_K.

8th Symposium on Prospects in the Physics of Discrete Symmetries (DISCRETE 2022)
7-11 November, 2022
Baden-Baden, Germany

*Speaker

PoS(DISCRETE2022)041

1. Introduction

Indirect CP violation in the neutral kaon system, parameterized by ϵ_K, is one of the most sensitive precision probes of new physics. The parameter ϵ_K can be expressed to excellent approximation as [1]

$$\epsilon_K \equiv e^{i\phi_\epsilon} \sin\phi_\epsilon \frac{1}{2} \arg\left(\frac{-M_{12}}{\Gamma_{12}}\right). \tag{1}$$

Here, $\phi_\epsilon = \arctan(2\Delta M_K/\Delta\Gamma_K)$, with ΔM_K and $\Delta\Gamma_K$ the mass and lifetime difference of the weak eigenstates K_L and K_S. M_{12} and Γ_{12} are the Hermitian and anti-Hermitian parts of the Hamiltonian that determines the time evolution of the neutral kaon system. The short-distance contributions to ϵ_K are then contained in the matrix element $M_{12} = -\langle K^0|\mathcal{L}_{f=3}^{\Delta S=2}|\bar{K}^0\rangle/(2\Delta M_K)$, up to higher powers in the operator-product expansion.

Experimentally, ϵ_K is well-known, with absolute value $|\epsilon_K| = (2.228 \pm 0.011) \times 10^{-3}$ and an uncertainty at the permil level [2]. The standard model (SM) contributions to neutral kaon mixing are conveniently described by the effective $|\Delta S| = 2$ Lagrangian with three active quark flavors,

$$\mathcal{L}_{f=3}^{|\Delta S|=2} = -\frac{G_F^2 M_W^2}{4\pi^2}\left[\lambda_u^2 C_{S2}''^{uu}(\mu) + \lambda_t^2 C_{S2}''^{tt}(\mu) + \lambda_u\lambda_t C_{S2}''^{ut}(\mu)\right] Q_{S2}'' + \text{h.c.} + \ldots, \tag{2}$$

valid at scales around $\mu = 2\,\text{GeV}$. Here,

$$Q_{S2}'' = \left(\bar{s}_L^\alpha \gamma_\mu d_L^\alpha\right) \otimes \left(\bar{s}_L^\beta \gamma^\mu d_L^\beta\right) \tag{3}$$

is the local $|\Delta S| = 2$ operator, where α and β are color indices, and the ellipsis denotes contributions of higher dimension local operators and non-local contributions of $|\Delta S| = 1$ operators. The reason for the appearance of the double primes will become clear later. The elements of the Cabibbo-Kobayashi-Maskawa (CKM) matrix are combined into the parameters $\lambda_i \equiv V_{is}^* V_{id}$. The long-distance SM contributions are comprised by the hadronic matrix element of the local $|\Delta S| = 2$ operator, and are given in terms of the kaon bag parameter $B_K = 0.7625(97)$ [3]. Long-distance contributions that are not included in B_K are parameterized by the correction factor $\kappa_\epsilon = 0.94(2)$ [4].

With theory uncertainties approaching the percent level, also parametrically smaller corrections have been taken into consideration recently. The power corrections to the effective Lagrangian [5] have been revisited in an extended analysis [6], leading to a one-percent increase of the SM prediction of ϵ_K. In these proceedings, we present the updated perturbative results including electroweak contributions given in Refs. [7, 8].

All diagrams have been calculated using self-written `FORM` [9] routines, implementing the two-loop recursion presented in Refs. [10, 11]. The amplitudes were generated using `qgraf` [12]. We perfomed several analytical checks throughout several stages of the calculations, as outlined in Refs. [7, 8].

2. Top-Quark Contribution

In this section, we calculate the coefficient $C_{S2}''^{tt}$, proportional to λ_t^2, to NLO in the electroweak interactions. This fixes the renormalization scheme of the electroweak input parameters contained

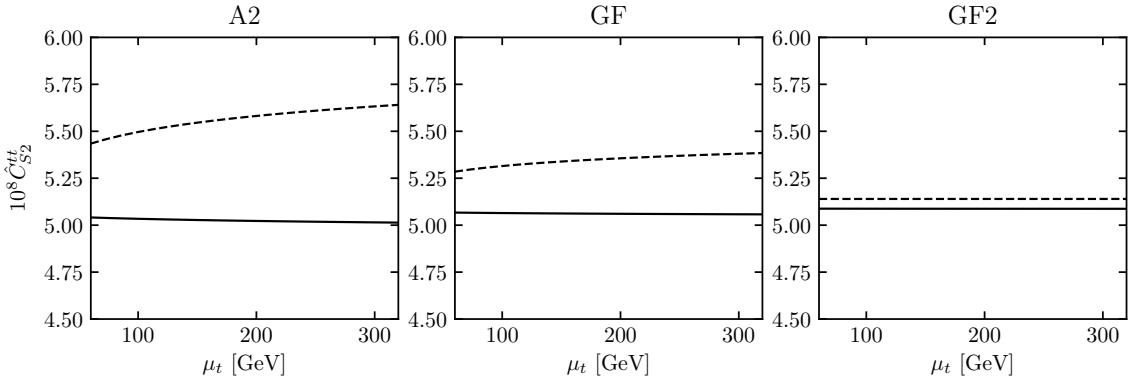

Figure 1: Residual electroweak matching scale dependence in the full OS scheme. The dashed line shows the LO result, while the solid line show the NLO result.

in the prefactor $G_F^2 M_W^2$. In fact, when only considering QCD effects, there are several equivalent ways of rewriting the prefactor, using the tree-level relation

$$G_F = \frac{\pi\alpha}{\sqrt{2} M_W^2 s_w^2}\,, \tag{4}$$

where $\alpha = e^2/(4\pi)$ the electromagnetic coupling and $s_w^2 = \sin^2\theta_w$ with the weak mixing angle θ_w. This choice specifies which experimental data are used as parametric input for our prediction. The numerical difference between the different schemes is expected to be large at LO, as exemplified by the 5% difference between the on-shell and $\overline{\text{MS}}$ values of s_w^2.

For our analysis of the top-quark contribution, it is useful to write the effective Lagrangian in the following form:

$$\mathcal{L}_{f=3}^{|\Delta S|=2} = \lambda_t^2 c_{S2}^{tt}(\mu) Q_{S2}^{(\prime,\prime\prime)} + \text{h.c.} + \ldots\,, \tag{5}$$

where the ellipsis now also includes contributions not proportional to λ_t^2. Using the tree-level relation (4), we express c_{S2}^{tt} in three different ways:

$$c_{S2}^{tt}(\mu) = -\frac{2\pi^2}{M_W^2 s_w^4} C_{S2}^{tt}(\mu)\,, \qquad c_{S2}^{tt}(\mu) = -\frac{G_F}{\sqrt{2} s_w^2} C_{S2}^{\prime tt}\,, \qquad c_{S2}^{tt}(\mu) = -\frac{G_F^2 M_W^2}{4\pi^2} C_{S2}^{\prime\prime tt}\,. \tag{6}$$

This effectively absorbs different parts of the radiative corrections into the measured value of the muon decay rate. In the first and second relation in Eq. (6) we have factored out the powers $(\alpha/(4\pi))^2$ and $\alpha/(4\pi)$, respectively, and absorbed them into rescaled operators, defined as

$$Q_{S2} = \left(\frac{\alpha}{4\pi}\right)^2 \left(\bar{s}_L^\alpha \gamma_\mu d_L^\alpha\right) \otimes \left(\bar{s}_L^\beta \gamma^\mu d_L^\beta\right), \tag{7}$$

and

$$Q_{S2}^\prime = \frac{\alpha}{4\pi} \left(\bar{s}_L^\alpha \gamma_\mu d_L^\alpha\right) \otimes \left(\bar{s}_L^\beta \gamma^\mu d_L^\beta\right), \tag{8}$$

while $Q_{S2}^{\prime\prime}$ has been defined in Eq. (3). With these conventions, the RG evolution is described by the same anomalous dimension in all three cases, and the LO values

$$C_{S2}^{tt}(\mu) = C_{S2}^{\prime tt}(\mu) = C_{S2}^{\prime\prime tt}(\mu) = S(x_t) \tag{9}$$

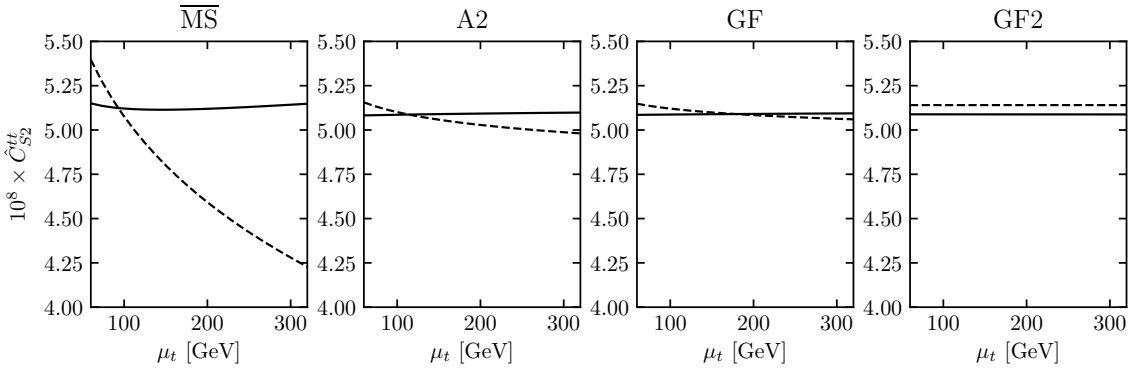

Figure 2: Residual electroweak matching scale dependence in the $\overline{\text{MS}}$ and hybrid schemes. The dashed line shows the LO result, while the solid line show the NLO result.

coincide. They are given by the modified [13] Inami-Lim box function [14]

$$\mathcal{S}(x_t) = \frac{4x_t - 11x_t^2 + x_t^3}{4(x_t-1)^2} + \frac{3x_t^3}{2(x_t-1)^3}\log x_t\,, \tag{10}$$

where $x_t \equiv m_t^2/M_W^2$, and we neglect a tiny correction of $O(m_c^2/M_W^2) \sim 10^{-4}$ [13]. We will refer to the first normalization in Eq. (6) as "A2", the second as "GF", and the third as "GF2". While, at LO in the weak interactions, the three parameterizations are equivalent, the numerical prediction depends on the chosen normalization and the scheme of the input parameters. These arbitrary dependences will be mitigated to a large degree by the NLO electroweak corrections.

Additionally, we considered several renormalization schemes for electroweak parameters to ensure we are using the scheme which shows the best perturbative convergence (the $\overline{\text{MS}}$ scheme is always used for electromagnetic and QCD gauge couplings):

1. On-Shell scheme: on-shell values used for all masses as well as s_w
2. $\overline{\text{MS}}$ scheme: $\overline{\text{MS}}$ values used for all masses as well as s_w
3. Hybrid scheme: on-shell values used for all masses and $\overline{\text{MS}}$ value used for s_w

As a note, in the $\overline{\text{MS}}$ scheme, only the A2 normalization for the EFT operator makes sense since G_F is inherently calculated using the on-shell scheme. As shown in Fig. 1, the on-shell scheme shows poor perturbative convergence, particularly due to the aforementioned large corrections to the on-shell value of s_w. From Fig. 2, we see that the hybrid scheme produces the best perturbative convergence, especially in the GF EFT normalization.

These results are then combined with the known NLO QCD results for C_{S2}^{tt} given in Ref. [15]. The residual dependence on the electroweak matching scale is shown in Fig. 3. We again see the most desirable perturbative behavior from the hybrid renormalization scheme for electroweak parameters. The results for the central values of the Wilson coefficients in the different EFT normalizations in the hybrid renormalization scheme are given in Tab. 1. The reported errors are calculated using the residual dependence on the electroweak matching scale. Noteably, we find that, after including NLL QED resummation effects, all EFT normalizations exactly coincide.

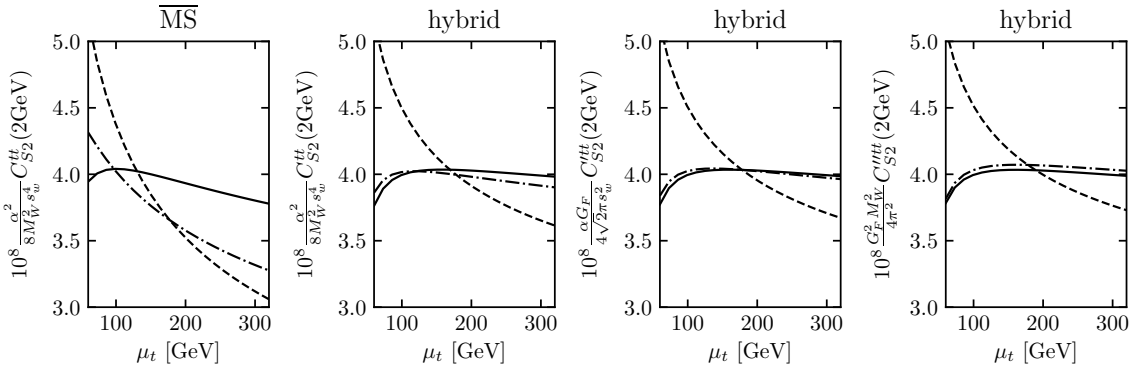

Figure 3: Residual matching scale dependence with full QCD resummation, in the $\overline{\text{MS}}$ and hybrid schemes. The dashed line shows the LO result, the dash-dotted line shows the result including NLO QCD corrections, while the solid line show the full (QCD and QED) NLO result.

	NLL QCD	NLL QCD & NLL QED
$\alpha^2/(8M_W^2 s_w^4) C_{S2}^{tt}(2\,\text{GeV}) \times 10^8$	3.96(6)	3.98(6)
$\alpha G_F/(4\sqrt{2}\pi s_w^2) C_{S2}^{\prime tt}(2\,\text{GeV}) \times 10^8$	4.00(4)	3.98(5)
$G_F^2 M_W^2/(4\pi^2) C_{S2}^{\prime\prime tt}(2\,\text{GeV}) \times 10^8$	4.02(5)	3.98(5)

Table 1: Wilson coefficients. Uncertainty given is scale variation only.

In the existing literature, the QCD results are presented in the GF2 normalization, which receives a -1% shift to the Wilson coefficient from electroweak corrections. Note that the GF normalization, this shift is halved.

3. Charm-Top Contribution

The LO result of the box diagrams proportional to $\lambda_u\lambda_t$ features a large logarithm $\sim x_c \log x_c$ which must be resummed in the EFT. This is accomplished by considering the mixing of $|\Delta S| = 1$ operators into the $|\Delta S| = 2$ operator in Eq. (5).

The Lagrangian (5) is valid below the charm-quark scale. Its Wilson coefficients are obtained by matching from the effective four- and five flavor Lagrangians

$$\begin{aligned}\mathcal{L}_{f=4,5}^{\text{eff}} = -\frac{4G_F}{\sqrt{2}}\left[\sum_{q,q'=u,c} V_{qs}^* V_{q'd}(C_+ Q_+^{qq'} + C_- Q_-^{qq'}) - \lambda_t \sum_{i=3,6} C_i Q_i\right] \\ - \frac{G_F^2 M_W^2}{4\pi^2}\lambda_t^2 C_{S2}^{tt} Q_{S2} - 8G_F^2\left(\lambda_u\lambda_t + \lambda_t^2\right)\tilde{C}_7\tilde{Q}_7 + \text{h.c.}\,,\end{aligned} \tag{11}$$

after the appropriate RG evolution, as described below. The first line in Eq. (11) contains the $|\Delta S| = 1$ current-current operators, defined as

$$Q_\pm^{qq'} = \frac{1}{2}\left((\bar{s}_L^\alpha \gamma_\mu q_L^\alpha)(\bar{q}_L'^\beta \gamma^\mu d_L^\beta) \pm (\bar{s}_L^\alpha \gamma_\mu q_L^\beta)(\bar{q}_L'^\beta \gamma^\mu d_L^\alpha)\right). \tag{12}$$

Here, α, β are $SU(3)$ color indices. The QCD-penguin operators Q_i, $i = 3, \ldots, 6$, are defined, e.g., in Ref. [16]. They are neglected in this work as they constitute a percent-level correction to our

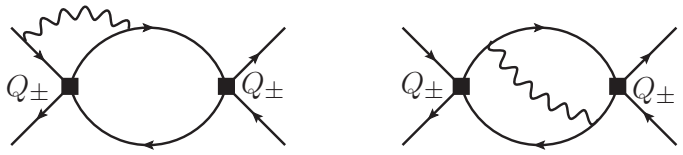

Figure 4: Sample Feynman diagrams with bilocal insertions of the current-current operators $Q_\pm^{qq'}$. Solid lines denote appropriate quark flavors, and wavy lines denote photons.

numerically small results (see Ref. [17]). The $|\Delta S| = 1$ operators mix, via bilocal insertions, into the local $|\Delta S| = 2$ operator, see Fig. 4. For the contributions proportional to $\lambda_u\lambda_t$, the Glashow-Iliopoulos-Maiani mechanism ensures that the mixing starts at order m_c^2; it is therefore convenient to define a rescaled version of the Q_{S2} operator as

$$\tilde{Q}_7 = \frac{m_c^2}{g_s^2\mu^{2\epsilon}}(\bar{s}_L\gamma_\mu d_L)(\bar{s}_L\gamma_\mu d_L)\,. \tag{13}$$

This operator is formally of dimension eight. The appearance of the strong coupling constant in the denominator takes account of the large logarithm in the LO result. The details of the RG running are given in Ref. [8] including the modified RGEs featuring the anomalous dimension tensor corresponding to the mixing of double-insertions of $|\Delta S| = 1$ operators into $\tilde{Q}_7$. After matching onto the three-flavor theory at the charm scale, μ_c, the running proceeds in an analogous way as C_{S2}^{tt}.

To obtain a numerical estimate of the size of the electroweak corrections, as well as an estimate of the remaining perturbative uncertainties, we evaluate the Wilson coefficient $\tilde{C}_{S2}^{ut}(2\,\text{GeV})$, including now all known QCD corrections, and varying the electroweak and charm-threshold matching scales in the intervals $40\,\text{GeV} \le \mu_t \le 320\,\text{GeV}$ and $1\,\text{GeV} \le \mu_c \le 2\,\text{GeV}$. (The dependence on the bottom-quark matching scale is negligible in comparison.) The resulting residual scale variation is displayed in Fig. 5.

To obtain a final value, we fix $\mu_t = m_t$ and take the average of the highest and lowest value of $\tilde{C}_{S2}^{ut}$ in the interval for the variation of μ_c, and half the difference between the highest and lowest values as the uncertainty. Retaining only the QCD corrections up to NNLL, we find $\tilde{C}_{S2}^{ut,\text{QCD}} = -13.84 \pm 0.17$. Including also the LL and NLL electroweak corrections gives $\tilde{C}_{S2}^{ut} = -13.92 \pm 0.16$. This amounts to a -0.5% shift, while the uncertainty is essentially unchanged.

4. Renormalization Scheme Dependence

One point that deserves discussion is the fact that our two-loop electroweak contributions to C_{S2}^{tt} and C_{S2}^{ut} are dependent on the definition of evanescent operators. The SM prediction for the physical observable ϵ_K must, of course, be independent of such arbitrary choices; in fact, the scheme dependence of the Wilson coefficient will cancel exactly against the corresponding scheme dependence of the hadronic matrix element. In the literature on ϵ_K, the scheme independent product of Wilson coefficient and matrix element is usually factorized into two *separately scheme- and scale-independent* quantities, namely, the QCD correction factors η_{tt} and η_{ut}, and the kaon bag factor $\hat{B}_K$. This is achieved by writing the evolution matrix as $U(\mu_0, \mu, \alpha) = K^{-1}(\mu_0, \alpha)U^{(0)}(\mu_0, \mu, \alpha)K(\mu, \alpha)$,

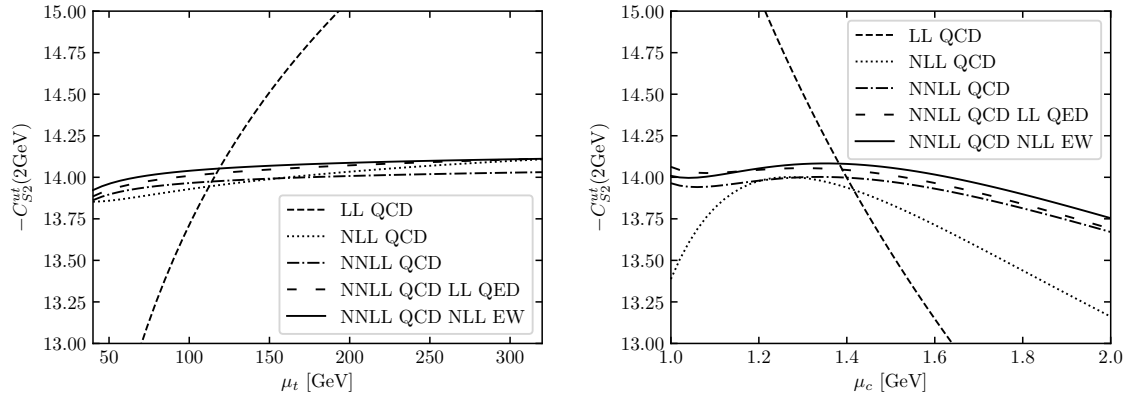

Figure 5: Residual dependence of the Wilson cofficient $\tilde{C}_{S2}^{ut}(2\,\text{GeV})$ on the electroweak (left panel) and charm-threshold (right panel) matching scales. The short-dashed, dotted, and dash-dotted lines show the LL, NLL, and NNLL QCD results, respectively. The long-dashed and solid lines show the results including also the LL and NLL electroweak corrections.

and combining the K factors, together with the appropriate part of the LO evolution matrix, with the Wilson coefficients and the matrix elements to yield scheme-independent quantities (see Refs. [18, 19] for details).

In our case, this strategy fails when including QED corrections, as the $O(\alpha\alpha_s)$ $|\Delta S| = 2$ anomalous dimension is scheme independent by itself. This is consistent with the general expression for the scheme dependence of anomalous dimensions given in Ref. [18], because here the anomalous dimension is a one-dimensional matrix, i.e. just a number. Therefore, the definition of the scheme-invariant correction factors cannot be extended to include QED effects (as a fixed-order expansion in α).

While a consistent estimate of the full electroweak and QED corrections can be obtained only once a lattice calculation (or another systematic estimate) of the QED correction to the hadronic matrix element becomes available, we point out that this correction is not enhanced by a large logarithm and thus of order $\alpha/(4\pi) \sim 10^{-4}$, the same as the residual scheme dependence. It is expected to be numerically negligible compared to the $O(1\%)$ shifts found above. It follows that for our numerics we can safely fix the definition of evanescent operators.

5. Conclusions

To summarize, given the uncancelled (but small) residual scheme dependence of our result, we propose a temporary prescription: we rescale the NLL QCD value of η_{tt} and NNLL QCD value of η_{ut} by factors of 0.99 and 1.005, respectively, to take account of the electroweak corrections. Including also the power correction presented in Ref. [6], this leads to an updated SM prediction of

$$|\epsilon_K| = \left(2.170 \pm 0.065_{\text{pert.}} \pm 0.076_{\text{nonpert.}} \pm 0.153_{\text{param.}}\right) \times 10^{-3}\,. \tag{14}$$

Here, the quoted errors correspond to the residual perturbative, non-perturbative, and parametric uncertainties, respectively; see Ref. [13] for details. We obtained this number by employing the

phenomenological expression in Ref. [19], including the long-distance corrections presented in Refs. [4, 20].

All parametric inputs are taken from PDG [21]. In particular, as input for the top-quark mass we use the $\overline{\text{MS}}$ mass $m_t(m_t) = 162.92(67)\,\text{GeV}$, obtained by converting the pole mass $M_t = 172.5(7)\,\text{GeV}$ [21] to $\overline{\text{MS}}$ at three-loop accuracy using RUNDEC [22].

Acknowledgements

The authors acknowledge support in part by DoE grant de-sc0011784. We also thanks Martin Gorbahn and Emmanuel Stamou for discussions.

References

[1] *B physics at the Tevatron: Run II and beyond*, 12, 2001.

[2] Particle Data Group collaboration, P. A. Zyla et al., *Review of Particle Physics*, *PTEP* **2020** (2020) 083C01.

[3] Flavour Lattice Averaging Group collaboration, S. Aoki et al., *FLAG Review 2019*, 1902.08191.

[4] A. J. Buras, D. Guadagnoli and G. Isidori, *On ϵ_K Beyond Lowest Order in the Operator Product Expansion*, *Phys. Lett. B* **688** (2010) 309–313, [1002.3612].

[5] O. Cata and S. Peris, *Long distance dimension eight operators in B(K)*, *JHEP* **03** (2003) 060, [hep-ph/0303162].

[6] M. Ciuchini, E. Franco, V. Lubicz, G. Martinelli, L. Silvestrini and C. Tarantino, *Power corrections to the CP-violation parameter ε_K*, *JHEP* **02** (2022) 181, [2111.05153].

[7] J. Brod, S. Kvedaraitė and Z. Polonsky, *Two-loop electroweak corrections to the Top-Quark Contribution to ϵ_K*, *JHEP* **12** (2021) 198, [2108.00017].

[8] J. Brod, S. Kvedaraite, Z. Polonsky and A. Youssef, *Electroweak corrections to the Charm-Top-Quark Contribution to ϵ_K*, *JHEP* **12** (2022) 014, [2207.07669].

[9] J. A. M. Vermaseren, *New features of FORM*, math-ph/0010025.

[10] A. I. Davydychev and J. B. Tausk, *Two loop selfenergy diagrams with different masses and the momentum expansion*, *Nucl. Phys.* **B397** (1993) 123–142.

[11] C. Bobeth, M. Misiak and J. Urban, *Photonic penguins at two loops and m_t dependence of $BR[B \to X_s l^+ l^-]$*, *Nucl. Phys. B* **574** (2000) 291–330, [hep-ph/9910220].

[12] P. Nogueira, *Automatic Feynman graph generation*, *J. Comput. Phys.* **105** (1993) 279–289.

[13] J. Brod, M. Gorbahn and E. Stamou, *Standard-Model Prediction of ϵ_K with Manifest Quark-Mixing Unitarity*, *Phys. Rev. Lett.* **125** (2020) 171803, [1911.06822].

[14] T. Inami and C. S. Lim, *Effects of Superheavy Quarks and Leptons in Low-Energy Weak Processes $K_L \to \mu\bar{\mu}$, $K^+ \to \pi^+\nu\bar{\nu}$, and $K^0 \leftrightarrow \bar{K}^0$*, *Prog. Theor. Phys.* **65** (1981) 297.

[15] A. J. Buras, M. Jamin and P. H. Weisz, *Leading and Next-to-leading QCD Corrections to ϵ Parameter and $B^0 - \bar{B}^0$ Mixing in the Presence of a Heavy Top Quark*, *Nucl. Phys. B* **347** (1990) 491–536.

[16] J. Brod and M. Gorbahn, *Epsilon_K at Next-to-Next-to-Leading Order: The Charm-Top-Quark Contribution*, *Phys. Rev. D* **82** (2010) 094026, [1007.0684].

[17] S. Herrlich and U. Nierste, *The Complete $|\Delta S| = 2$ Hamiltonian in the next-to-leading order*, *Nucl. Phys. B* **476** (1996) 27–88, [hep-ph/9604330].

[18] A. J. Buras, M. Jamin and M. E. Lautenbacher, *The Anatomy of ϵ'/ϵ beyond leading logarithms with improved hadronic matrix elements*, *Nucl. Phys. B* **408** (1993) 209–285, [hep-ph/9303284].

[19] G. Buchalla, A. J. Buras and M. E. Lautenbacher, *Weak decays beyond leading logarithms*, *Rev. Mod. Phys.* **68** (1996) 1125–1144, [hep-ph/9512380].

[20] *B physics at the Tevatron: Run II and beyond*, 12, 2001.

[21] Particle Data Group collaboration, R. L. Workman, *Review of Particle Physics*, *PTEP* **2022** (2022) 083C01.

[22] K. G. Chetyrkin, J. H. Kuhn and M. Steinhauser, *RunDec: A Mathematica package for running and decoupling of the strong coupling and quark masses*, *Comput. Phys. Commun.* **133** (2000) 43–65, [hep-ph/0004189].

PoS(DISCRETE2022)041